

Thermally-Enhanced Fröhlich Coupling in SnSe

Fabio Caruso, Maria Troppenz, Santiago Rigamonti, and Claudia Draxl

Institut für Physik and IRIS Adlershof, Humboldt-Universität zu Berlin, Berlin, Germany

(Dated: May 23, 2019)

To gain insight into the peculiar temperature dependence of the thermoelectric material SnSe, we employ many-body perturbation theory and explore the influence of the electron-phonon interaction on its electronic and transport properties. We show that a lattice dynamics characterized by soft highly-polar phonons induces a large thermal enhancement of the Fröhlich interaction. We account for these phenomena in ab-initio calculations of the photoemission spectrum and electrical conductivity at finite temperature, unraveling the mechanisms behind recent experimental data. Our results reveal a complex interplay between lattice thermal expansion and Fröhlich coupling, providing a new rationale for the *in-silico* prediction of transport coefficients of high-performance thermoelectrics.

The discovery of the record-breaking thermoelectric properties of SnSe has laid a new milestone in the quest for high-efficiency thermoelectric materials [1]. SnSe combines large carrier conductivity σ and Seebeck coefficient S , with highly anharmonic lattice dynamics [2–4]. Anharmonic effects limit the lattice thermal conductivity κ via phonon-phonon scattering, thus contributing to a record-high figure of merit $ZT = (S^2\sigma/\kappa)T \sim 2.6$, which may be even further improved through doping and alloying [5–8].

As the operational conditions of thermoelectric devices typically involve large temperatures, a quantum-mechanical description of the electronic and lattice properties of SnSe across the temperature domain of its thermodynamical stability is key to unravel the microscopic origin of this outstanding thermoelectric performance. Recent experimental investigations have unveiled a pervasive influence of temperature on the electronic and transport properties of SnSe. Angle-resolved photoemission spectroscopy experiments, for instance, have reported (i) a pronounced dependence of the peak linewidth on the sample temperature [9], (ii) the emergence at low temperature of a gap between the first two occupied bands at the Z point, [10–13], and (iii) a non-monotonic effective-mass renormalization as a function of temperature [14]. Density-functional theory calculations fail at unraveling the origin of these phenomena. Additionally, theoretical predictions based on the Boltzmann formalism indicate an increase of the electrical conductivity with temperature – arising from the thermal excitation of carriers across the Fermi surface – which is in stark contrast with experimental observations, where a pronounced reduction of charge conduction with increasing temperature has been observed [5].

These findings seem to suggest a strong interplay between electronic and ionic degrees of freedom. While recent theoretical works have thus far provided a comprehensive investigation, based on first-principles calculations, of quasiparticle bands [15], defect formation energies [16], crystal-lattice dynamics [17], lattice anharmonicities [4], electron-phonon interaction [18], and

transport properties [15, 19, 20], unraveling the origin of the peculiar temperature-dependent properties of this high-performance thermoelectric continues to represent a major challenge.

In this work, we tackle the temperature-induced renormalization of the electronic and transport properties of SnSe by combining, within a first-principles framework, the many-body theory of the electron-phonon interaction in the Fan-Migdal approach and the Boltzmann transport formalism beyond the constant relaxation time, including effects of the lattice expansion. We find a strong enhancement of the electron-phonon coupling strength with temperature which stems from the thermal excitation of soft polar modes and manifests itself through band-structure renormalization effects, an increase of electron linewidths by a factor of five between 0 and 600 K, and a highly-anisotropic renormalization of the hole effective mass. Our first-principles calculations of the electrical conductivity are in excellent agreement with experiments, and demonstrate the importance of accounting simultaneously for the temperature-dependence of the scattering time due to electron-phonon interaction and the thermal expansion of the crystal lattice. Overall, our results unveil a complex interplay between lattice anharmonicities and electron-phonon coupling which underpins the microscopic origin of the temperature-dependent properties of SnSe, paving the way towards the study of transport phenomena in thermoelectric materials.

SnSe crystallizes in a layered orthorhombic structure of the $Pnma$ space group [21]. Its phonon dispersion, as obtained from density-functional perturbation theory (DFPT), is illustrated in Fig. 1 (a) for momenta along the high-symmetry line $Y-\Gamma-Z$ in the Brillouin zone. Phonons have been computed for the relaxed crystal structure at zero temperature. SnSe is characterized by soft polar phonon modes with energies smaller than 25 meV (202 cm^{-1}). The polar character of the optical phonons manifests itself through the discontinuity in their energy at Γ and is quantified by large average Born effective charges (-3.8 for Sn and 3.8 for Se, in good agreement with previous calculations [2]). In Fig. 1 (b) and (c) ar-

rows illustrate the atomic displacements corresponding to the B_u and B_g modes, marked by red dots in Fig. 1 (a), which exemplify the lattice dynamics induced by polar phonons in SnSe. A comprehensive characterization of the optical phonon modes is provided in the Supplemental Material [22].

The pronounced polar character of SnSe suggests that the effects of electron-phonon interaction may be important. Additionally, since the energy scales of the optical modes are comparable to the room-temperature thermal energy $k_B T \simeq 25$ meV, the population of low-energy phonons, governed by the Bose-Einstein distribution $n_{\mathbf{q}\nu} = [\exp(\hbar\omega_{\mathbf{q}\nu}/k_B T) - 1]^{-1}$, is subject to a strong temperature dependence, which may lead to a significant thermal enhancement of the electron-phonon interaction. To investigate these aspects on a quantitative ground, we perform first-principles calculations of the electron-phonon interaction by evaluating the electron self-energy in the Fan-Migdal approximation as:

$$\Sigma_{n\mathbf{k}}(\omega) = \int \frac{d\mathbf{q}}{\Omega_{\text{BZ}}} \sum_{m\nu} |g_{m\nu}(\mathbf{k}, \mathbf{q})|^2 \quad (1)$$

$$\times \left[\frac{n_{\mathbf{q}\nu} + f_{m\mathbf{k}+\mathbf{q}}}{\hbar\omega - \tilde{\varepsilon}_{m\mathbf{k}+\mathbf{q}} + \hbar\omega_{\mathbf{q}\nu}} + \frac{n_{\mathbf{q}\nu} + 1 - f_{m\mathbf{k}+\mathbf{q}}}{\hbar\omega - \tilde{\varepsilon}_{m\mathbf{k}+\mathbf{q}} - \hbar\omega_{\mathbf{q}\nu}} \right].$$

Here $n_{\mathbf{q}\nu}$ and $f_{n\mathbf{k}}$ are Bose-Einstein and Fermi-Dirac occupation factors for phonons and electrons, respectively. $\tilde{\varepsilon}_{n\mathbf{k}} = \varepsilon_{n\mathbf{k}} + i\eta$, where $\varepsilon_{n\mathbf{k}}$ are Kohn-Sham (KS) single particle energies, η is a positive infinitesimal, and $\omega_{\mathbf{q}\nu}$ are phonon frequencies. $g_{m\nu}(\mathbf{k}, \mathbf{q}) = \langle \psi_{m\mathbf{k}+\mathbf{q}} | \Delta_{\mathbf{q}\nu} V_{\text{KS}}(\mathbf{r}) | \psi_{n\mathbf{k}} \rangle$ are the electron-phonon coupling matrix elements, where $\Delta_{\mathbf{q}\nu} V_{\text{KS}}$ denotes the change of the effective KS potential upon a phonon displacement with momentum \mathbf{q} and index ν , and $\psi_{n\mathbf{k}}$ are KS orbitals. The polar character of the electron-phonon matrix elements $g_{m\nu}(\mathbf{k}, \mathbf{q})$ due to the Fröhlich interaction is accounted for following the first-principles method of Ref. [23]. Equation (1) has been evaluated within the EPW code [24]. All computational details are provided in the Supplemental Material [22].

The Eliashberg function $\alpha^2 F(\omega)$ for doped SnSe (here and below we consider a p -type doping concentration of $4 \cdot 10^{19} \text{ cm}^{-3}$), shown in Fig. 1 (d) reflects the weighted phonon density of states, to which individual phonons contribute according to their electron-phonon coupling strength [25]. $\alpha^2 F(\omega)$ exhibits a sharp peak at 20 meV, which arises from the B_g mode marked by red dots in Fig. 1 (a). This feature accounts for about 50% of the total electron-phonon coupling strength $\lambda = 2 \int_0^\infty d\omega \alpha^2 F(\omega) / \omega$, suggesting that the coupling between electrons and phonons stems primarily from this mode. This scenario is reminiscent of highly-doped oxides, such as, e.g., TiO_2 and EuO , where the formation of distinctive polaronic satellites in the angle-resolved spectral function [26, 27] has been attributed to the coupling to a single polar phonon [23, 28, 29].

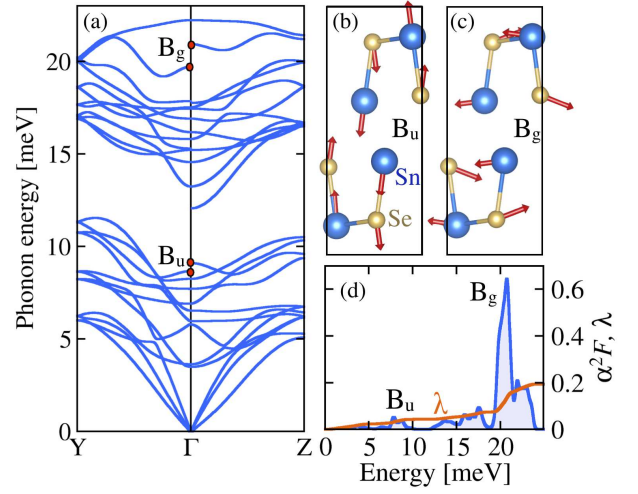


Figure 1. (a) Phonon dispersion as obtained from DFPT. (b)-(c) Eigenvectors of the polar phonons B_u and B_g , respectively, marked by red dots in (a). (d) Eliashberg function and cumulative electron-phonon coupling strength λ for doped SnSe.

We now proceed to investigate the temperature dependence of the electronic structure. In Fig. 2 (a)-(f), we show the angle-resolved spectral function due to the electron-phonon interaction in the diagonal approximation,

$$A_{n\mathbf{k}}(\omega) = -\frac{1}{\pi} \frac{\text{Im}\Sigma_{n\mathbf{k}}(\omega)}{[\hbar\omega - \varepsilon_{n\mathbf{k}} - \text{Re}\Sigma_{n\mathbf{k}}(\omega)]^2 + [\text{Im}\Sigma_{n\mathbf{k}}(\omega)]^2} \quad (2)$$

at 80 and 600 K for undoped SnSe. Numerical results for intermediate temperatures (298 and 450 K) are reported in the Supplemental Material [22]. We consider paths parallel to the three crystallographic directions, passing through the valence-band maximum (VBM) at $(0, 0, 0.26) \text{ \AA}^{-1}$. The single-particle energies obtained from DFT band-structure calculations (light blue) are included for comparison. All energies are relative to the VBM.

As compared to Eq. (2), the cumulant expansion approach provides a more suitable formalism to describe photoemission satellites [30]. At variance with highly-doped oxides, however, which exhibit signatures of low-energy plasmonic and polaronic satellites in ARPES [23, 26, 29, 31, 32], SnSe does not reveal such effects, thus, validating a description of its spectral properties within the Fan-Migdal approximation.

The comparison of the spectral function obtained from Eqs. (1)-(2) to the DFT band structure, where the electron-phonon interaction is neglected, reveals a pronounced temperature-dependent renormalization of the electronic structure. In the low-temperature regime (80 K), the quasiparticle peaks are broadened by the interaction with phonons, reflecting the finite lifetimes of photo-excited holes in the valence band. However, the spectrum exhibits only a small renormalization of the

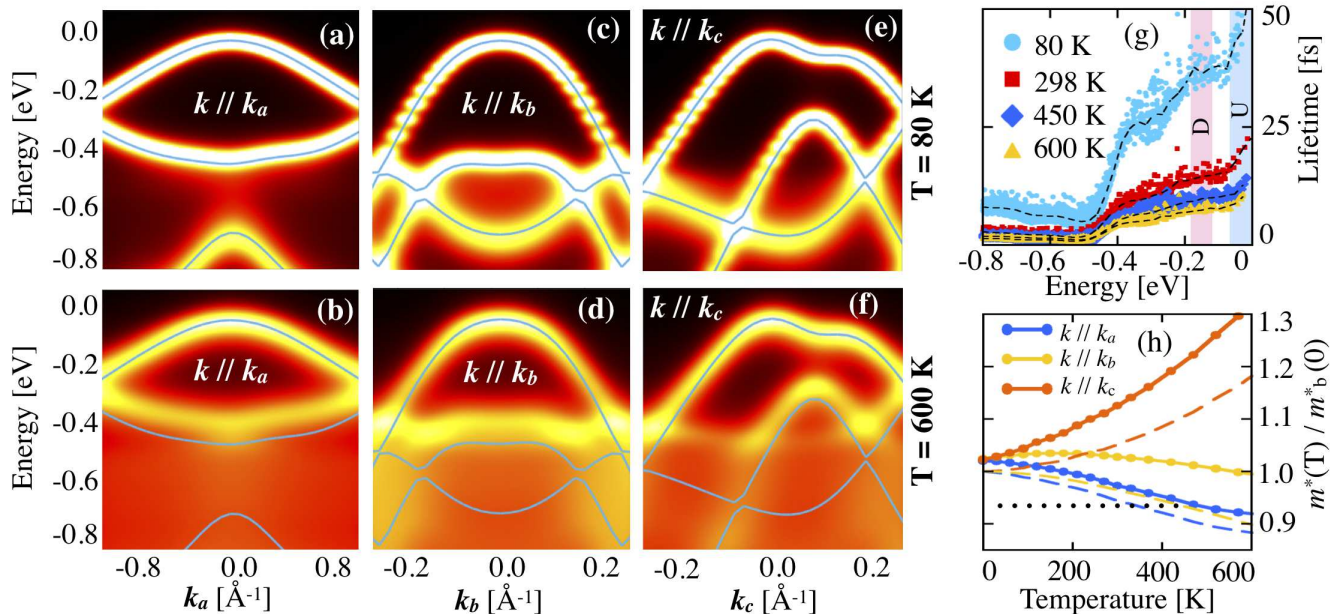


Figure 2. Temperature dependence of the angle-resolved spectral function for the valence bands for crystal momenta along the \mathbf{k}_x [(a)-(b)], \mathbf{k}_y [(c)-(d)], and \mathbf{k}_z [(e)-(f)] directions in the Brillouin zone. The DFT bands (light blue) are superimposed for comparison. Discrete features in panels (c) and (e) are an artifact resulting from finite crystal-momentum resolution. (g) Hole lifetime as a function of charge-carrier energies at 80, 298, 450, and 600 K. The isotropic average at a given energy is shown by dashed lines, whereas the shaded areas indicate energy windows of 50 meV, corresponding to the thermal energy $k_B T$ at 600 K for undoped (U) and doped (D) SnSe. (h) Temperature-dependent renormalization of the effective mass along the three crystal axes. The bare DFT effective masses $m_b^*(T)$ are shown by dashed lines.

quasiparticle energies, as indicated by their overlap with the DFT bands.

The increase of temperature to 600 K is accompanied by a significant enhancement of the electron linewidths and of the quasiparticle energy renormalization. The linewidth is more pronounced for binding energies larger than 0.4 eV. This behaviour, which is in line with recent ARPES experiments performed at room temperature, is dictated by the onset of the $4p$ -Se bands, which enlarges the phase-space available for the decay of photo-excited holes. At these binding energies, we obtain electron linewidths ranging between 0.2 and 0.4 eV. As they become comparable to the energy separation between different valence states, the identification of distinct quasiparticle bands is obstructed by the large peak broadening, and the spectral features merge together into a broad background. These results suggest a breakdown of the quasiparticle picture at high temperatures, whereby a transition to a strong electron-phonon coupling regime is induced by the thermal excitation of soft polar modes.

To further investigate the influence of temperature on the electronic properties, we evaluate the effective-mass renormalization due to the combined effect of (i) the electron-phonon interaction and (ii) the anisotropic thermal expansion of the crystal lattice [33]. To account for these effects, we obtain the effective mass from [25]:

$$m^*(T) = m_b^*(T)[1 + \lambda_{n\mathbf{k}}(T)]. \quad (3)$$

In this expression, m_b^* is the bare effective mass extracted from the DFT band structure. Its temperature dependence stems from the thermal expansion of the lattice induced by anharmonic effects, which are accounted for by employing at each temperature the experimental crystal structure [33]. The necessity of accounting for lattice anharmonicities in SnSe has previously been suggested in Ref. [20], whereby the use of temperature-dependent crystal structures has proven important to obtain accurate Seebeck coefficients. The coupling to phonons is included via the electron-phonon coupling strength $\lambda_{n\mathbf{k}} = -\hbar^{-1} \partial \Sigma_{n\mathbf{k}}(\omega) / \partial \omega|_{\varepsilon_F}$ with ε_F being the Fermi energy, and n, \mathbf{k} denoting the band and momentum index corresponding to the valence band top.

The temperature dependence of m_b^* and m^* relative to $m_b^*(T = 0)$ is illustrated in Fig. 2 (h). In the low-temperature limit, our calculations yield $m_b^*(0) = 0.69, 0.34,$ and $0.16 m_e$ along $a, b,$ and $c,$ respectively, where m_e is the electron mass, in good agreement with earlier calculations [15]. The thermal expansion of the lattice leads to a monotonic decrease of $m_b^*(T)$ with increasing temperature for momenta along the reciprocal lattice vectors \mathbf{k}_a and \mathbf{k}_b . The opposite trend observed along \mathbf{k}_c stems from the negative thermal expansion of the lattice in this direction [33]. The inclusion of the electron-phonon interaction systematically enhances the effective mass with temperature, owing to

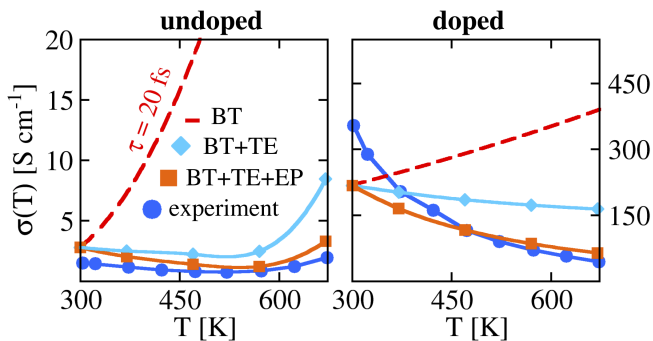


Figure 3. Electrical conductivity along the crystallographic axis a for undoped (left) and doped (right) SnSe obtained using the Boltzmann transport equation (BT) with a constant relaxation time $\tau = 20$ fs; BT with thermal expansion of the lattice (BT+TE); and combining BT with thermal expansion and temperature-dependent τ due to electron-phonon coupling (BT+TE+EP). Experimental data (circles) are from Ref. [5].

the increase of the phonon population via thermal excitation. While the effective-mass renormalization due to the lattice expansion and the coupling to phonons sums up along \mathbf{k}_c , these effects partially cancel out in the \mathbf{k}_a and \mathbf{k}_b directions. Remarkably, along \mathbf{k}_b the interplay of lattice anharmonicity and electron-phonon coupling leads to a distinctive maximum of the effective mass at around 160 K, a trend in good agreement with recent ARPES measurements [14]. Overall, these results reveal a complex interplay of lattice anharmonicity and electron-phonon interactions which underpins a highly anisotropic temperature-dependent modulation of the effective mass. Lattice anharmonicities and finite temperature effects may further influence the electron-phonon interaction via the change of the phonon dispersion for the thermally expanded structure. While finite temperature calculations have been addressed in the past [34, 35], accounting for such effects in *ab-initio* studies of the electron-phonon interaction is still a challenge.

The hole lifetimes, obtained as $\tau_{n\mathbf{k}} = \hbar/2\text{Im}\Sigma_{n\mathbf{k}}$, and illustrated in Fig. 2 (g) as a function of carrier energy for temperatures between 80 and 600 K, further provide a quantitative estimation of the characteristic timescales for the relaxation of excited holes, which is critical to infer the temperature-dependence of the transport properties. The shaded region indicates the energy window of thermally excited carriers which take part in transport phenomena at 600 K for undoped and doped SnSe. Close to the Fermi energy, we obtain lifetimes of the order of 45-50 fs at 80 K, which drop below 10 fs at 600 K. The temperature-induced suppression of carrier dynamics is much more pronounced than in non-polar semiconductors and insulators, as e.g., diamond [36, 37] and silicon [38, 39]. For binding energies larger than 0.4 eV, Fig. 2 (g) illustrates a further suppression of the relax-

ation time, down to 8 fs (1 fs) at 80 K (600 K).

Finally, to investigate how temperature affects the transport properties, we evaluate the electrical conductivity σ via the linearized Boltzmann equation in the relaxation time approximation [40]:

$$\sigma = \frac{e^2}{m_e^2} \sum_{n\mathbf{k}} \left(- \frac{\partial f}{\partial \epsilon} \Big|_{\epsilon_{n\mathbf{k}}} \right) \mathbf{p}_{n\mathbf{k}} \mathbf{p}_{n\mathbf{k}} \tau_{n\mathbf{k}}. \quad (4)$$

Here, $\mathbf{p}_{n\mathbf{k}} = -i\hbar\langle\psi_{n\mathbf{k}}|\nabla|\psi_{n\mathbf{k}}\rangle$ is the momentum matrix element of the electronic state with band index n and wave vector \mathbf{k} , f the Fermi-Dirac distribution function, and $\tau_{n\mathbf{k}}$ the carrier scattering time. In the following, we approximate $\tau_{n\mathbf{k}}$ by the isotropic average of the relaxation time at the Fermi surface. Calculations based on Eq. (4) are performed for undoped and doped SnSe, using the `exciting` code [41] (all computational details are reported in the Supplemental Material [22]) [42], and compared to measurements from Ref. [5]. For the undoped SnSe, we assume a hole concentration of $4.5 \cdot 10^{17} \text{ cm}^{-3}$ to account for the additional carriers induced by the formation of Sn vacancies [20]. The results obtained for the crystallographic axis \mathbf{a} are shown in Fig. 3.

If the temperature dependence of the relaxation time is neglected (setting $\tau = 20$ fs) in Eq. (4), the standard expression for the conductivity Boltzmann transport (BT) of both undoped and hole-doped SnSe increases with temperature owing to the enhanced population of thermally-excited holes. This behavior, which is in striking contrast with experiment [5], is ameliorated by taking into account the thermal lattice expansion at each temperature (BT+TE, squares in Fig. 3). However, a good quantitative agreement with the experimental conductivity is only recovered by simultaneously accounting for lattice anharmonicities and the temperature-dependent renormalization of the relaxation time due to the electron-phonon interaction (BT+TE+EP). The residual difference between theory and experiment is ascribed to uncertainties in the determination of the hole concentrations and to additional coupling mechanisms, such as, e.g., impurity, electron-electron, and electron-plasmon scattering [43], neglected in our calculations. Overall, our results indicate that, beside influencing pervasively the spectral properties, the thermal enhancement of the polar-phonon population is also responsible for the temperature-induced suppression of hole transport.

In conclusion, we have investigated the influence of temperature on the electronic and transport properties of SnSe by accounting for the coupling between electrons, phonons, and lattice anharmonicities within a first-principles many-body framework. At finite temperature the electronic structure exhibits thermally-enhanced electron linewidths, a suppression of hole relaxation times, and a highly-anisotropic renormalization of the hole effective masses. These phenomena are attributed to the

coexistence of soft polar phonons and large Born effective charges, which induce a strong increase of the electron-phonon interaction between 0 and 600 K. Accounting simultaneously for the thermal expansion of the lattice and electron-phonon interaction is key to explain the temperature dependence of recent experimental data for the electrical conductivity. Overall, a sizeable thermal enhancement of the electron-phonon interaction may constitute a general feature of compounds characterized by low-energy phonons with large Born effective charges such as, e.g., other Pb- and Sn-chalcogenides [44–46]. This study reveals the crucial importance of accounting for these processes to accurately describe transport phenomena in high-performance thermoelectrics.

Discussions with Dino Novko are gratefully acknowledged. MT acknowledges funding from the Elsa-Neumann Scholarship of Berlin.

-
- [1] L.-D. Zhao, S.-H. Lo, Y. Zhang, H. Sun, G. Tan, C. Uher, C. Wolverton, V. P. Dravid, and M. G. Kanatzidis, *Nature* **508**, 373 (2014).
- [2] C. W. Li, J. Hong, A. F. May, D. Bansal, S. Chi, T. Hong, G. Ehlers, and O. Delaire, *Nature Phys.* **11**, 1063 (2015).
- [3] L.-D. Zhao, C. Chang, G. Tan, and M. G. Kanatzidis, *Energy Environ. Sci.* **9**, 3044 (2016).
- [4] J. M. Skelton, L. A. Burton, S. C. Parker, A. Walsh, C.-E. Kim, A. Soon, J. Buckeridge, A. A. Sokol, C. R. A. Catlow, A. Togo, and I. Tanaka, *Phys. Rev. Lett.* **117**, 075502 (2016).
- [5] L.-D. Zhao, G. Tan, S. Hao, J. He, Y. Pei, H. Chi, H. Wang, S. Gong, H. Xu, V. P. Dravid, C. Uher, G. J. Snyder, C. Wolverton, and M. G. Kanatzidis, *Science* (2015).
- [6] W. Wei, C. Chang, T. Yang, J. Liu, H. Tang, J. Zhang, Y. Li, F. Xu, Z. Zhang, J.-F. Li, and G. Tang, *J. Am. Chem. Soc.* **140**, 499 (2018).
- [7] T.-R. Wei, G. Tan, X. Zhang, C.-F. Wu, J.-F. Li, V. P. Dravid, G. J. Snyder, and M. G. Kanatzidis, *J. Am. Chem. Soc.* **138**, 8875 (2016).
- [8] T.-R. Wei, G. Tan, C.-F. Wu, C. Chang, L.-D. Zhao, J.-F. Li, G. J. Snyder, and M. G. Kanatzidis, *Appl. Phys. Lett.* **110**, 053901 (2017).
- [9] Q. Lu, M. Wu, D. Wu, C. Chang, Y.-P. Guo, C.-S. Zhou, W. Li, X.-M. Ma, G. Wang, L.-D. Zhao, L. Huang, C. Liu, and J. He, *Phys. Rev. Lett.* **119**, 116401 (2017).
- [10] T. Nagayama, K. Terashima, T. Wakita, H. Fujiwara, T. Fukura, Y. Yano, K. Ono, H. Kumigashira, O. Ogiso, A. Yamashita, Y. Takano, H. Mori, H. Usui, M. Ochi, K. Kuroki, Y. Muraoka, and T. Yokoya, *Jpn. J. Appl. Phys.* **57**, 010301 (2018).
- [11] V. Tayari, B. V. Senkovskiy, D. Rybkovskiy, N. Ehlen, A. Fedorov, C.-Y. Chen, J. Avila, M. Asensio, A. Perucchi, P. di Pietro, L. Yashina, I. Fakih, N. Hemsworth, M. Petrescu, G. Gervais, A. Grüneis, and T. Szkopec, *Phys. Rev. B* **97**, 045424 (2018).
- [12] Z. Wang, C. Fan, Z. Shen, C. Hua, Q. Hu, F. Sheng, Y. Lu, H. Fang, Z. Qiu, J. Lu, Z. Liu, W. Liu, Y. Huang, Z.-A. Xu, D. W. Shen, and Y. Zheng, *Nature Comm.* **9**, 47 (2018).
- [13] C. W. Wang, Y. Y. Y. Xia, Z. Tian, J. Jiang, B. H. Li, S. T. Cui, H. F. Yang, A. J. Liang, X. Y. Zhan, G. H. Hong, S. Liu, C. Chen, M. X. Wang, L. X. Yang, Z. Liu, Q. X. Mi, G. Li, J. M. Xue, Z. K. Liu, and Y. L. Chen, *Phys. Rev. B* **96**, 165118 (2017).
- [14] M. Maeda, K. Yamamoto, T. Mizokawa, N. L. Saini, M. Arita, H. Namatame, M. Taniguchi, G. Tan, L. D. Zhao, and M. G. Kanatzidis, *Phys. Rev. B* **97**, 121110 (2018).
- [15] G. Shi and E. Kioupakis, *J. Appl. Phys.* **117**, 065103 (2015).
- [16] Y. Huang, C. Wang, X. Chen, D. Zhou, J. Du, S. Wang, and L. Ning, *RSC Adv.* **7**, 27612 (2017).
- [17] R. Guo, X. Wang, Y. Kuang, and B. Huang, *Phys. Rev. B* **92**, 115202 (2015).
- [18] J. Ma, Y. Chen, and W. Li, *Phys. Rev. B* **97**, 205207 (2018).
- [19] K. Kutorasinski, B. Wiendlocha, S. Kaprzyk, and J. Tobola, *Phys. Rev. B* **91**, 205201 (2015).
- [20] A. Dewandre, O. Hellman, S. Bhattacharya, A. H. Romero, G. K. H. Madsen, and M. J. Verstraete, *Phys. Rev. Lett.* **117**, 276601 (2016).
- [21] A. N. Mariano and K. L. Chopra, *Appl. Phys. Lett.* **10**, 282 (1967).
- [22] See Supplemental Material at [tobeaddedbypublisher](#) which includes Refs. [47–54].
- [23] C. Verdi, F. Caruso, and F. Giustino, *Nat. Commun.* **8**, 15769 (2017).
- [24] S. Poncé, E. Margine, C. Verdi, and F. Giustino, *Comput. Phys. Commun.* **209**, 116 (2016).
- [25] G. Grimvall, *The electron-phonon interaction in metals*, Selected topics in solid state physics (North-Holland, 1981).
- [26] S. Moser, L. Moreschini, J. Jaćimović, O. S. Barišić, H. Berger, A. Magrez, Y. J. Chang, K. S. Kim, A. Bostwick, E. Rotenberg, L. Forró, and M. Grioni, *Phys. Rev. Lett.* **110**, 196403 (2013).
- [27] S. Moser, S. Fatale, P. Krüger, H. Berger, P. Bugnon, A. Magrez, H. Niwa, J. Miyawaki, Y. Harada, and M. Grioni, *Phys. Rev. Lett.* **115**, 096404 (2015).
- [28] J. M. Riley, F. Caruso, C. Verdi, L. B. Duffy, M. D. Watson, L. Bawden, K. Volckaert, G. van der Laan, T. Hesjedal, M. Hoesch, F. Giustino, and P. D. C. King, *Nature Comm.* **9**, 2305 (2018).
- [29] F. Caruso, C. Verdi, S. Poncé, and F. Giustino, *Phys. Rev. B* **97**, 165113 (2018).
- [30] B. Gumhalter, V. Kovač, F. Caruso, H. Lambert, and F. Giustino, *Phys. Rev. B* **94**, 035103 (2016).
- [31] Z. Wang, S. McKeown Walker, A. Tamai, Y. Wang, Z. Ristic, F. Y. Bruno, A. de la Torre, S. Riccò, N. C. Plumb, M. Shi, P. Hlawenka, J. Sánchez-Barriga, A. Varykhalov, T. K. Kim, M. Hoesch, P. D. C. King, W. Meevasana, U. Diebold, J. Mesot, B. Moritz, T. P. Devereaux, M. Radovic, and F. Baumberger, *Nat. Mater.* **15**, 835 (2016).
- [32] F. Borgatti, J. A. Berger, D. Céolin, J. S. Zhou, J. J. Kas, M. Guzzo, C. F. McConville, F. Offi, G. Panaccione, A. Regoutz, D. J. Payne, J.-P. Rueff, O. Bierwagen, M. E. White, J. S. Speck, M. Gatti, and R. G. Egdell, *ArXiv e-prints* (2017), arXiv:1710.08829 [cond-mat.str-el].
- [33] D. Bansal, J. Hong, C. W. Li, A. F. May, W. Porter, M. Y. Hu, D. L. Abernathy, and O. Delaire,

- Phys. Rev. B **94**, 054307 (2016).
- [34] O. Hellman, I. A. Abrikosov, and S. I. Simak, Phys. Rev. B **84**, 180301 (2011).
- [35] O. Hellman, P. Steneteg, I. A. Abrikosov, and S. I. Simak, Phys. Rev. B **87**, 104111 (2013).
- [36] S. Logothetidis, J. Petalas, H. M. Polatoglou, and D. Fuchs, Phys. Rev. B **46**, 4483 (1992).
- [37] F. Giustino, S. G. Louie, and M. L. Cohen, Phys. Rev. Lett. **105**, 265501 (2010).
- [38] P. Lautenschlager, P. B. Allen, and M. Cardona, Phys. Rev. B **33**, 5501 (1986).
- [39] S. Poncé, Y. Gillet, J. Laflamme Janssen, A. Marini, M. Verstraete, and X. Gonze, J. Chem. Phys. **143**, 102813 (2015).
- [40] T. J. Scheidemantel, C. Ambrosch-Draxl, T. Thonhauser, J. V. Badding, and J. O. Sofo, Phys. Rev. B **68**, 125210 (2003).
- [41] A. Gulans, S. Kontur, C. Meisenbichler, D. Nabok, P. Pavone, S. Rigamonti, S. Sagmeister, U. Werner, and C. Draxl, Journal of Physics: Condensed Matter **26**, 363202 (2014).
- [42] Input and output files are available online at <http://dx.doi.org/10.17172/NOMAD/2018.10.10-1>.
- [43] F. Caruso and F. Giustino, Phys. Rev. B **94**, 115208 (2016).
- [44] Y. Zhang, X. Ke, C. Chen, J. Yang, and P. R. C. Kent, Phys. Rev. B **80**, 024304 (2009).
- [45] Z. Tian, J. Garg, K. Esfarjani, T. Shiga, J. Shiomi, and G. Chen, Phys. Rev. B **85**, 184303 (2012).
- [46] R. Guo, X. Wang, Y. Kuang, and B. Huang, Phys. Rev. B **92**, 115202 (2015).
- [47] P. Hohenberg and W. Kohn, Phys. Rev. **136**, B864 (1964).
- [48] W. Kohn and L. J. Sham, Phys. Rev. **140**, A1133 (1965).
- [49] P. Giannozzi *et al.*, J. Phys.: Condens. Matter **21**, 395502 (2009).
- [50] J. P. Perdew, K. Burke, and M. Ernzerhof, Phys. Rev. Lett. **77**, 3865 (1996).
- [51] N. Troullier and J. L. Martins, Phys. Rev. B **43**, 1993 (1991).
- [52] S. Baroni, S. de Gironcoli, A. Dal Corso, and P. Giannozzi, Rev. Mod. Phys. **73**, 515 (2001).
- [53] N. Marzari, A. A. Mostofi, J. R. Yates, I. Souza, and D. Vanderbilt, Rev. Mod. Phys. **84**, 1419 (2012).
- [54] A. A. Mostofi, J. R. Yates, Y.-S. Lee, I. Souza, D. Vanderbilt, and N. Marzari, Comput. Phys. Commun. **178**, 685 (2008).